ESM APPENDIX S2: ANALYSES OF COLONIZATION HISTORY AND TIME-FOR-SPECIATION

1) Ancestral range estimation using BioGeoBEARS

a. Extended Methods

i. BioGeoBEARS

In order to determine the number of colonizations of each region and their timing, we reconstructed ancestral regions using the Dispersal-Extinction-Cladogenesis framework (DEC; [1]) implemented in the R package *BioGeoBEARS* version 0.2.1 (with extra functionality downloaded from http://phylo.wdfiles.com using the source() function on June 20, 2017; [2]). We used the OBIS/GBIF dataset to assign all 4,571 species in the phylogeny to one or more of eight marine regions. We chose the OBIS/GBIF dataset over alternatives (see appendix S1) because this is the only geographic dataset that included all species of Percomorpha (over 17,000 species). This dataset also allowed us to estimate total richness in each region, including species that were not sampled in the phylogeny (table S2). The maximum range size of ancestral species was set to 9, meaning that a single ancestral species could co-occur in all 9 regions (which was true for 5 extant species). We did not include the null range (i.e. we fit the DEC* model of Massana et al. [3]), meaning that we did not allow anagenic transitions to "no" regions. Simulations show that excluding the null range in the anagenic transition matrix generally improves ancestral-area reconstruction and estimation of local extinction rates, which are often underestimated under the DEC model [3]. Although founder-effect speciation is possible for marine organisms [4], preliminary analyses showed that the DEC*+J model implementing jump dispersal (cladogenic dispersal between areas instead of anagenic dispersal and extinction) had a relatively poorer fit to our data (ΔAIC > 4; [5]).

We followed Cowman and Bellwood [6] and Dornburg et al. [7] in restricting dispersal across time and space as follows. When relevant, we used their dates and dispersal probabilities in order to maintain consistency with previous studies of historical biogeography of fishes. In all time strata, dispersal was only allowed between contiguous areas. For example, dispersal was allowed between NC and EP, but not NC and SC. The latter change would require anagenetic dispersal and local extinction within a third area. The probability of dispersal between CP and EP was set to 0.05 (following previous authors) across all time strata to represent the East Pacific Barrier. We set the probability of dispersal between WA and EA to 0.05 after 60 Ma to represent the Mid-Atlantic Barrier [8]. We reduced dispersal between EA and WI to 0.05 after 18 Ma to represent the closure of the Tethys Seaway and limited dispersal around the Horn of Africa. Finally, we allowed dispersal between EP and WA until 3.1 Ma to represent the final closure of the Isthmus of Panama (dates from [6,7]). In all time bins, habitat transitions between marine and freshwater were possible from all marine regions, but occurred at a low relative frequency (0.05) reflecting physiological constraints [9]. While habitat transitions are thought to be more frequent in fishes than other organisms [9], these transitions still seem to be more difficult than dispersal among marine regions, justifying our restricted probability of dispersal here. Time-stratified matrices and all other input files can be downloaded from the Dryad package associated with this study.

ii. Additional constraints informed by the fossil record

Our biogeographic analyses are based on the geographic ranges of extant taxa. However, the fossil record of marine fishes shows that many groups originated in the Tethys (present-day East Atlantic; [10,11]). Further, the CIP was much less productive prior to ~34 million years ago (Ma) compared to the present, and may have been unsuitable for reef fishes [11]. If these Tethys inhabitants did not leave any extant descendants in the region, then our reconstructions may not reflect ancient Tethys occupation. This may bias our results if colonizations of the CIP are inferred to be older than they actually were, which may lead to inflated support for the time-for-speciation effect. For example, the crown of some reef-fish families may be reconstructed in the CIP instead of the Tethys as supported by the fossil record [7].

To account for this possible bias, we performed a second set of ancestral-area reconstructions with additional constraints informed by the fossil record. In these analyses we constrained relevant nodes to occur in the EA, and prevented the occupation of the CIP prior to 34 Ma to reflect its unsuitability for reef fishes. To determine which nodes to constrain, we investigated the phylogenetic relationships and ages (based on [12]) of extant families with Tethys fossils listed in Table 1 of Bellwood et al. [10], which is based on Bannikov [13]. This fossil deposit is found in the present-day East Atlantic (Monte Bolca, Italy) and represents a Tethys assemblage from 50 Ma. It was difficult to determine the exact nodes corresponding to fossil taxa for several reasons: (i) phylogenetic sampling was poor for many groups; (ii) some fossils represent extinct genera with unclear phylogenetic affinities; and (iii) the crown ages of some extant groups with fossil representatives were much younger than 50 Ma.

For these reasons, we assumed that families with Monte Bolca fossils originated in the Tethys, which is reasonable for many groups (i.e. Monte Bolca fossils represent the first appearances in the fossil record for several families). For these families, we constrained the crown age and internal nodes older than 34 Ma to occur in the EA. We constrained the stem node for monotypic families, families with a sister clade that also occurred in the Tethys, and families where the crown age was younger than 34 Ma. For all constrained nodes, we also excluded the CIP and CP regions. In addition, across the phylogeny we prevented colonization of the CIP until 34 Ma. These constraints together correspond to the “hopping hotspots” pattern described by Renema et al. [11]. In this model, the Tethys was the hotspot of diversity during the Eocene, while the present-day CIP and adjacent CP had low diversity. The period starting at 34 Ma (Oligocene boundary) represents a shift in diversity from the Tethys to the CIP, corresponding to an increase in carbonate platforms and shallow water due to tectonic activity. Constrained nodes are shown in table S3.

This constrained reconstruction model makes two assumptions that are difficult to confirm due to the general lack of fossil evidence. First, we are assuming that all families with fossil representatives in the Tethys actually originated there. Second, we are assuming that none of these families extended into the present-day CIP and CP before 34 Ma because of a lack of suitable habitat. In reality, these assumptions may be true for some families but not others. Thus, this model should be treated as an extreme case, suitable to test the greatest possible bias on our

results caused by performing biogeographic reconstructions on extant taxa only. We emphasize again that our goal in performing these constrained reconstructions is to assess possible biases (i.e. increasing support for the time-for-speciation effect) that are caused by the lack of fossil taxa. They are not intended as a definitive statement about the biogeographic origins of marine fish families.

iii. Detecting and dating colonizations

In both sets of reconstructions, to count colonizations along the phylogeny and to incorporate uncertainty in the ancestral-state reconstructions in downstream analyses, we simulated 100 independent biogeographic histories ("stochastic maps") conditional on the observed distributional data, phylogeny, and fitted DEC* model [14]. This provided 100 possible histories of area colonization given the phylogeny, extant geographic ranges, and likelihood. Results are reported as mean values among the 100 maps.

The time-for-speciation effect depends on identifying the timing of colonization(s) of a region [15]. For each stochastic map, a colonization of a region was detected when a node or terminal taxon was reconstructed with an area different from that of its parent node (tip ranges are known from our geographic dataset). Under a DEC model, colonizations may only occur via anagenetic range expansion (range shifts are allowed in a DEC+J model, but this model had poor fit to our data). Note that we counted and dated colonizations at nodes and not branches. This is because a colonization event can occur anywhere along a branch subtended by a parent node, but must be no younger than the descendant node. In cases where colonizations were inferred within terminal taxa (judged in comparison to their parent node), we assumed the event occurred at one-half the length of the terminal branch. Violations of this assumption are unlikely to change our results, because monotypic colonizations tend to be young, and so the range of possible colonization times is small. General types of colonizations and their detection are illustrated in figure S2.

Our overall procedure for estimating the timing of colonization could generate two main sources of error. First, we will always underestimate the age of colonizations, because events actually occurred along the branch subtending the descendant node. However, this is unlikely to provide spurious support for the time-for-speciation effect, because this bias should reduce the inferred time to build up richness in each region. Second, we will not detect colonizations that left no descendants in a region. Specifically, to colonize a non-contiguous region, a lineage must first expand its range to include an intermediate region, and may then go locally extinct in that region (see figure S2). In this scenario, the colonization to the intermediate region will not be detected at a descendant node. This is also unlikely to produce spurious support for the time-for-speciation effect because no descendants of this colonization will remain in the intermediate region (i.e. the event does not contribute to regional richness). Furthermore, our detection criteria are applied consistently to all regions, so these sources of error should not bias our results to favor greater time in any particular region.

iv. Assessing the effect of missing taxa using Labridae

Biogeographic models (i.e. DEC) do not implement a correction for missing species in the phylogeny. The 2013 phylogeny used here [12] contains 4,571 species of percomorph fishes, all with genetic data. A very recently published phylogeny now includes ~6,800 percomorph species with genetic data [16]. This provides an opportunity to test how our colonization results may change with additional phylogenetic sampling.

We repeated our biogeographic reconstructions on three tree types: (i) the 2013 tree ([12] used in in our main analyses), (ii) the 2018 tree including only those taxa with genetic data [16], and (iii) a set of 100 trees from the 2018 paper [16] with missing species added semi-randomly using taxonomic constraints ("all taxa added" or "ATA" phylogenies of [16]). We did this on the subset of the phylogenies corresponding to Labridae (wrasses and parrotfishes). Note that our use of Labridae here includes Scaridae and Odacidae, because this is a monophyletic lineage, but these families are still recognized by FishBase. Labrids are a focal group in many studies of reef fish biogeography [17,18], and are among the most diverse reef fish groups, with 630 described species (FishBase). They also show a similar richness gradient to all percomorphs (figure S7), with a peak in the CIP, moderate richness in the CP and WI, and low richness in the Atlantic and East Pacific. We used FishBase to resolve taxonomic incongruencies among phylogenies and remove synonyms. Afterwards, the 2013 tree contained 244 species of labrids, and the 2018 tree contained 339 species of labrids with genetic data. There are 100 fully-resolved trees that contained all 630 labrids after taxonomic verification, downloaded from fishtreeoflife.org on 12 August 2018.

We fit a DEC model to each phylogeny as described above (without fossil constraints, since our goal was simply to assess effects of missing taxa). There are no exclusively freshwater labrids, and only four species were endemic to the cold regions (*Odax pullus*, *Pseudolabrus miles*, and *Notolabrus cinctus* in SC; *Tautogolabrus adspersus* in NC). Therefore, to reduce computation time we excluded cold regions and freshwater from these reconstructions, leaving only the six warm marine regions. For the four coldwater species, we assigned their ranges to the closest warm-ocean regions (CP and WA respectively) based on FishBase. We set a maximum range area of 5 regions for each ancestral node (the maximum number of regions observed for any one extant species). Finally, for each phylogeny, we performed 100 stochastic map simulations based on the fitted DEC model, and calculated the number of colonizations and summed time-for-speciation as described in the main text and in this appendix.

For each of the three alternative tree types, the mean values of the number of colonizations and summed time-for-speciation among 100 stochastic maps are shown in figure S7. Statistical results are summarized in table S7. Results are similar among trees. Labrids show similar patterns to those from our analyses across all percomorphs: the number of colonizations and summed time are strongly and positively related to regional richness, and these relationships only become stronger with improved taxon sampling. For both the 2013 tree and 2018 tree with genetic data, the CP has more colonizations and summed time than the CIP although it has lower richness (different from results for all percomorphs, figure 2). The increase in the number of

species between these two trees (244 vs. 339) increased the overall number of colonizations to each region, but the rank-order of regions is identical between trees for both colonization number and summed time-for-speciation. This similarity suggests that adding more species should not overturn our conclusions about the causes of richness patterns based on biogeographic reconstructions, and may even strengthen our conclusions.

Performing biogeographic reconstructions on phylogenies with missing taxa added randomly (or semi-randomly) is potentially highly problematic. This is because clades descended from a single colonization event may be artificially broken up in a randomly resolved tree, incorrectly inflating the number of colonization events inferred (see also [19]). Nevertheless, we compared the results using reconstructions among the ATA phylogenies. We could only perform stochastic mapping on 67 of 100 trees. Stochastic simulations failed for the other 33 trees, most likely because of complications caused by very short branch lengths. The relationships between richness and colonization are still highly significant in ATA trees (table S7). Results among these 67 phylogenies are very similar to each other (figure S7). The only major difference between the ATA phylogenies and the two phylogenies based on genetic data is that the CIP exceeded the CP in the number of colonizations and summed time in the ATA phylogenies. However, we cannot know to what extent these extra colonizations are real versus an artifact of the random addition of species. The CIP has the lowest proportional sampling among the six warm marine regions. Specifically, 53% of labrid species in the CIP have genetic data in the 2018 phylogeny, versus 61–86% in the other regions (figure S7). Therefore, the CIP is expected to be more greatly affected than the other regions by artifacts from the random resolution of polytomies for genetically unsampled taxa.

Importantly, our overall conclusion in this study is that the CIP has more colonization events and greater summed time than other regions (figure 1). These analyses suggest that any bias in the reconstructions from our main results (using the 2013 tree) caused by incomplete sampling should result in underestimating the number of colonizations in the CIP, not overestimating them. Thus our main results appear to be conservative, given that the observed relationships become stronger with greater sampling.

In summary, these analyses using labrids suggest that: (i) increased phylogenetic sampling will increase the number of inferred colonization events in general, (ii) increased sampling should not overturn our conclusion that the CIP has more colonizations and greater summed time than other regions, and that the processes driving richness differences among regions are adequately captured by the 2013 phylogeny, and (iii) incomplete taxon sampling should not increase the risk of type-1 error (spurious relationship between richness and colonization) in our main results.

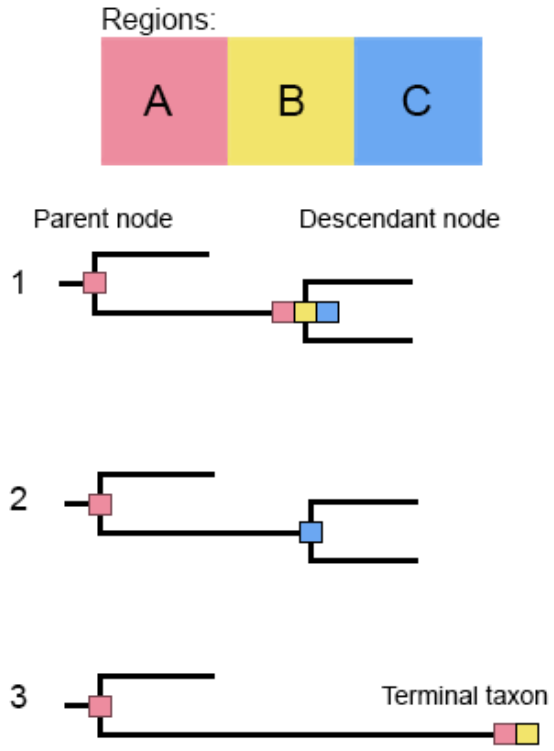

	Anagenetic processes	Recorded events
1	Range expansion to B and C	Colonization of B and C
2	Range expansion to B and C; Local extinction in A and B	Colonization of C
3	Range expansion to B	Colonization of B

Figure S2. General examples of colonization events and their detection in this study. In this scenario, regions A, B, and C are contiguous, with B in between A and C. In a DEC model, colonization is only achieved by anagenetic range expansion. Dispersal from A to C is not possible without range expansion to B. In this study, we counted independent colonization events if a descendant node or terminal taxon occurred in a new region compared to its parent node. Dispersal events that did not leave descendants were not counted (e.g. region B in example 2).

Table S3. Nodes constrained to occur in the East Atlantic (and excluding CIP and CP). Constraints are based on [10,13]. Crown and stem groups and their ages are based on [12]; ages of families are shown in database S2. We did not constrain any nodes younger than 34 Ma, including crown groups. Note that we did not constrain some families with Tethys fossils in [10]. We did not constrain the families Latidae and Percichthyidae because all extant members are freshwater (and thus not likely to bias our inference of colonization to the CIP). We did not constrain the families Brachionichthyidae and Solenostomidae because they were not included in the phylogeny we used. We did not include Ophidiidae because it is very old and undersampled, and so it seems unlikely that the extant species sampled have origins in the Tethys around 50 Ma.

Number	Group	Nodes constrained	Notes
1	Siganidae	Stem	Sister contains Tetraodontiformes, which also has Tethys fossils; crown is too young to assign to Tethys based on fossil record
2	Scatophagidae	Stem	Sister contains Tetraodontiformes, which also has Tethys fossils; crown is too young to assign to Tethys based on fossil record
3	Caproidae	Stem and crown	Sister contains Tetraodontiformes, which also has Tethys fossils
4	Triacanthidae	Stem	Sister also has Tethys fossils; crown is too young to assign to Tethys based on fossil record
5	Aracanidae + Ostraciidae	Clade crown (stem of each family)	Sister families that both have Tethys fossils; both family crowns are too young to assign to Tethys based on fossil record
6	Diodontidae + Tetraodontidae	Clade crown (stem of each family), and all nodes >34 Ma (includes crown of Tetraodontidae)	Sister families that both have Tethys fossils; crown of Diodontidae is too young to assign to Tethys based on fossil record
7	Lophiidae + Antennariidae	Clade crown (stem of each family) and all nodes >34 Ma (includes crown of both families)	Sister families that both have Tethys fossils
8	Ogcocephalidae	Stem	Crown is too young to assign to Tethys based on fossil record

9	Pomacentridae	Crown and all nodes >34 Ma	
10	Labridae	Crown and all nodes >34 Ma	Note that Scaridae and Odacidae are subsumed within paraphyletic Labridae, though they do not have Tethys fossils
11	Scombridae	Crown and all nodes >34 Ma	
12	Atherinidae	Crown and all nodes >34 Ma	
13	Monodactylidae	Stem	Monotypic family
14	Sparidae	Crown and all nodes >34 Ma	
15	Sphyraenidae	Crown and all nodes >34 Ma	
16	Apogonidae	Crown and all nodes >34 Ma	
17	Hemiramphidae + Exocoetidae	Clade crown and all nodes > 34 Ma (includes crown of both families)	Exocoetidae is subsumed within paraphyletic Hemiramphidae; both families have Tethys fossils
18	Carangidae	Crown and all nodes >34 Ma	
19	Priacanthidae	Crown and all nodes >34 Ma	
20	Gerreidae	Crown and all nodes >34 Ma	
21	Syngnathidae	Stem, crown, and all nodes >34 Ma	Sister group also contains Tethys fossils
22	Centriscidae + Aulostomidae	Clade crown and all nodes > 34 Ma (includes stem and crown of both families)	Sister families that both have Tethys fossils
23	Leiognathidae	Crown and all nodes	

		>34 Ma	
24	Lutjanidae	Clade crown and all nodes > 34 Ma	Note that Caesionidae is subsumed within paraphyletic Lutjanidae, though it does not have Tethys fossils
25	Acropomatidae	Clade crown and all nodes > 34 Ma	
26	Ephippidae	Stem	Crown is too young to assign to Tethys based on fossil record
27	Zanclidae + Acanthuridae	Clade crown (stem of both families) and all nodes > 34 Ma (includes crown of Acanthuirdae)	Sister families that both have Tethys fossils; Zanclidae is monotypic
28	Pomatomidae + Centrolophidae	Clade crown (stem of both families)	Sister families that both have Tethys fossils; Pomatomidae is monotypic; crown of Centrolophidae is too young to assign to Tethys based on fossil record
29	Menidae	Stem	Monotypic family

2. Extended results of time-for-speciation analyses

Table S4. Results of linear regressions of colonization metrics and regional richness across 100 stochastic maps, for the entire history of Percomorpha, and during two significant periods of reef evolution [10]. For each of 100 stochastic maps, we performed linear regressions of log10-transfomed regional richness (table S2) and two metrics of colonization history: the summed crown ages of each colonization to a region, and the number of colonizations to each region. Results are summarized as the means and standard deviations across 100 stochastic maps, and the number of maps (among 100) with a significant relationship. Freshwater was removed in one case because it was an outlier in the relationship between regional richness and number of colonizations (see figures 1, S3). Results with mean *P*-values<0.05 are in bold.

	No fossil constraints						Fossil constraints					
	Summed time			Number of colonization events			Summed time			Number of colonization events		
Comparison (number of regions)	Mean *P*	Mean r^2	Maps with *P*<0.05	Mean *P*	Mean r^2	Maps with *P*<0.05	Mean *P*	Mean r^2	Maps with *P*<0.05	Mean *P*	Mean r^2	Maps with *P*<0.05
All events (9)	0.455 ± 0.078	0.085 ± 0.026	0	0.118 ± 0.022	0.314 ± 0.030	0	0.339 ± 0.053	0.133 ± 0.026	0	0.068 ± 0.011	0.402 ± 0.024	6
All events, freshwater removed (8)	**0.002 ± 0.002**	**0.847 ± 0.051**	**100**	**0.002 ± 0.003**	**0.846 ± 0.055**	**100**	**0.002 ± 0.002**	**0.831 ± 0.040**	**100**	**<0.001 ± 0.000**	**0.911 ± 0.023**	**100**
34–5.3 Ma only (9)	**<0.001 ± 0.000**	**0.859 ± 0.049**	**100**	**<0.001 ± 0.000**	**0.845 ± 0.037**	**100**	**<0.001 ± 0.000**	**0.886 ± 0.042**	**100**	**<0.001 ± 0.000**	**0.918 ± 0.029**	**100**
5.3–0 Ma only (9)	**0.002 ± 0.002**	**0.786 ± 0.059**	**100**	**0.003 ± 0.003**	**0.765 ± 0.068**	**100**	**0.002 ± 0.001**	**0.795 ± 0.058**	**100**	**0.002 ± 0.002**	**0.792 ± 0.069**	**100**

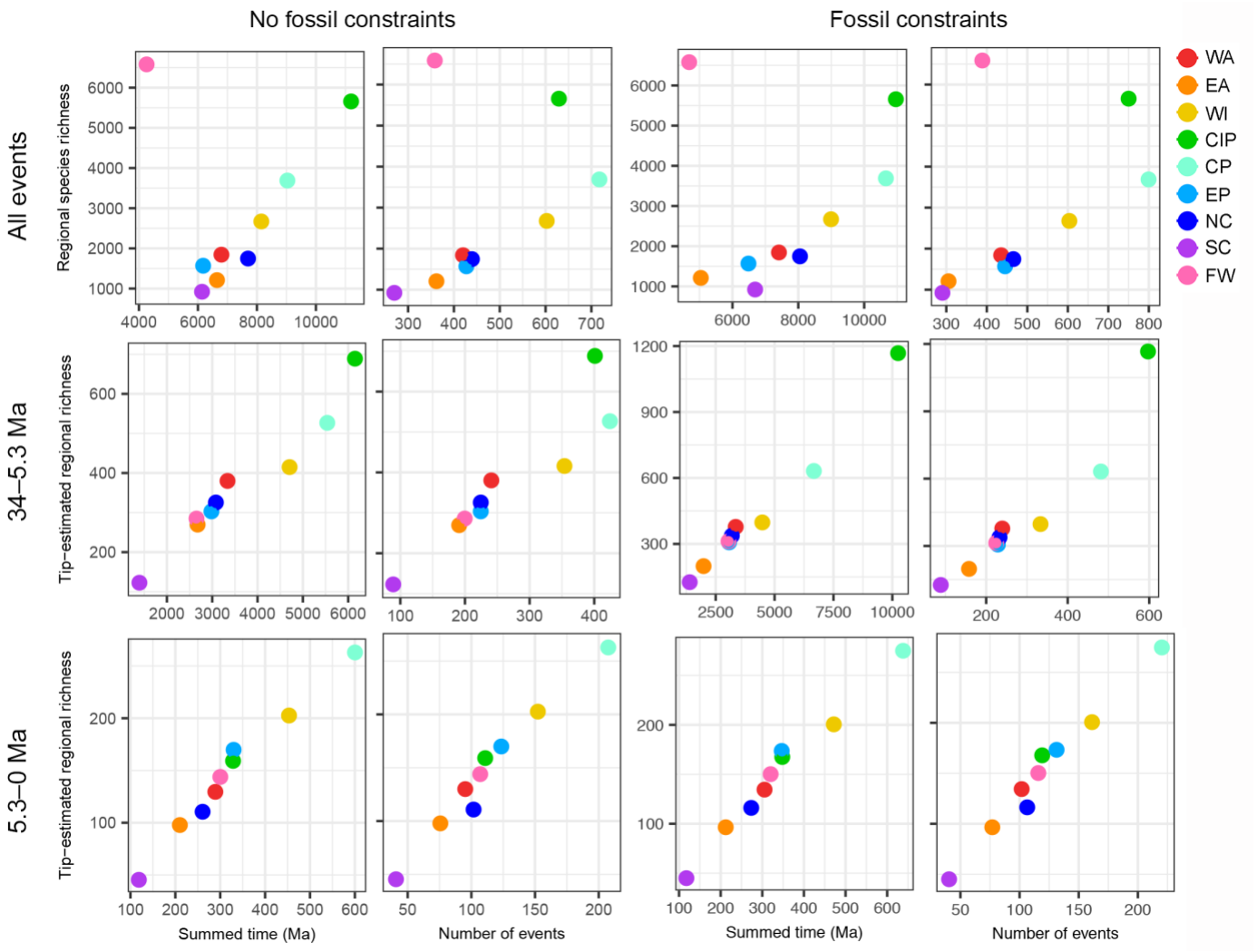

Figure S3. Regression between regional richness and two metrics of colonization history, for all events and during two significant periods of reef fish history [10]. Fossil constraints are shown in table S3 and described in Extended Methods. For analyses within time bins, the tip-estimated regional richness is the number of terminal taxa descended from colonization events occurring in the time period of interest (unsampled species could not be assigned to events occurring at a set time). Values are the means across 100 stochastic maps. See table S4 for significance values.

Table S5. Results of time-for-speciation analyses across the entire history of Percomorpha, and during two significant periods of reef evolution [10], for combined marine regions. To test the robustness of our results to alternative biogeographic comparisons, we combined the WA and EA into a single Atlantic region, and combined the WI, CIP, and CP into a single Indo-West Pacific region (all other regions are unchanged). We performed these analyses using ancestral reconstructions without fossil constraints. Regressions were performed as described in table S4. Freshwater was removed in one case because it was an outlier in the relationship between regional richness and number of colonization events (see figure S4). Results with mean *P*-values<0.05 are in bold.

	Summed time			Number of colonization events		
Comparison (number of regions)	Mean *P*	Mean r^2	Maps with *P*<0.05	Mean *P*	Mean r^2	Maps with *P*<0.05
All events, combined (7)	0.277 ± 0.016	0.283 ± 0.015	0	0.154 ± 0.006	0.435 ± 0.010	0
All events, combined, freshwater removed (6)	**0.007 ± 0.002**	**0.937 ± 0.011**	**100**	**0.003 ± 0.000**	**0.965 ± 0.004**	**100**
34–5.3 Ma, combined (7)	**0.016 ± 0.008**	**0.808 ± 0.054**	**100**	**0.015 ± 0.008**	**0.813 ± 0.053**	**100**
5.3–0 Ma, combined (7)	**0.015 ± 0.005**	**0.807 ± 0.030**	**100**	**0.015 ± 0.005**	**0.812 ± 0.032**	**100**

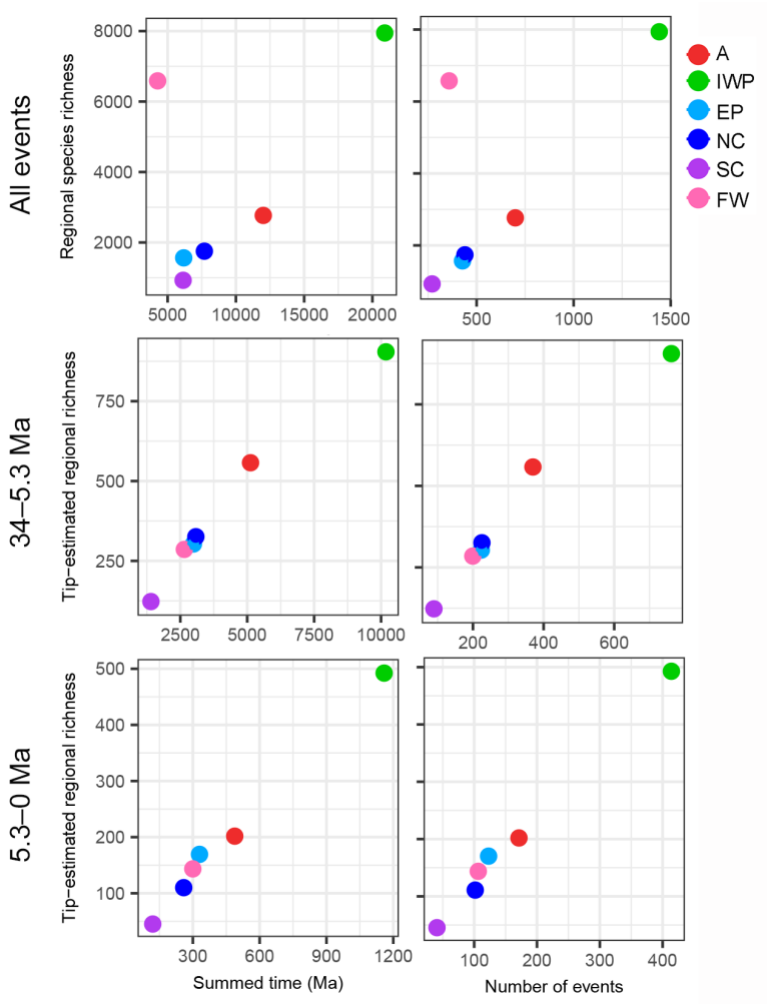

Figure S4. Regression between regional richness and two metrics of colonization history using combined regions. Here, A=Atlantic (WA+EA) and IWP=Indo-West Pacific (WI+CIP+CP). We performed these alternative analyses using ancestral reconstructions without fossil constraints. For analyses within time bins, the tip-estimated regional richness is the number of terminal taxa descended from colonizations occurring in the time period of interest (unsampled species could not be assigned to events occurring at a set time). Values are the means across 100 stochastic maps. See table S5 for significance values.

Figure S5. Number of colonizations of each region separated by source region (all events). If a region was colonized by a widespread lineage (parent lineage occurring in more than one region), then all regions of the parent lineage are shown as source regions. Mean number of events across 100 stochastic maps are shown. See figure S2 for details of detecting colonizations. Fossil constraints are described in the Extended Methods and table S3.

Table S6. Proportion of extant species in each region derived from novel colonizations (range expansion), versus those derived from in-situ speciation. Values are the means across 100 stochastic maps. The proportion of colonizers is the proportion of terminal taxa found in the region with a parent node not reconstructed in the region. The proportion of in-situ diversifiers is the inverse proportion (parent node was reconstructed in the region). Proportions are consistent with results in the main text (i.e. many taxa in the CIP derived from older colonizations; figure 2). Note that these values generally represent the most recent colonizations (those associated with terminal taxa) and not colonizations occurring deeper in the phylogeny.

	WA	EA	WI	CIP	CP	EP	NC	SC	FW
No fossil constraints									
Proportion colonizers	0.39	0.38	0.62	0.30	0.50	0.44	0.31	0.41	0.12
Proportion in-situ	0.61	0.62	0.38	0.70	0.50	0.56	0.69	0.59	0.88
Standard deviation	0.02	0.02	0.02	0.01	0.02	0.02	0.01	0.03	0
Fossil constraints									
Proportion colonizers	0.40	0.35	0.59	0.38	0.56	0.46	0.32	0.41	0.14
Proportion in-situ	0.60	0.65	0.41	0.62	0.44	0.54	0.68	0.59	0.86
Standard deviation	0.02	0.02	0.02	0.01	0.02	0.02	0.01	0.03	0.01

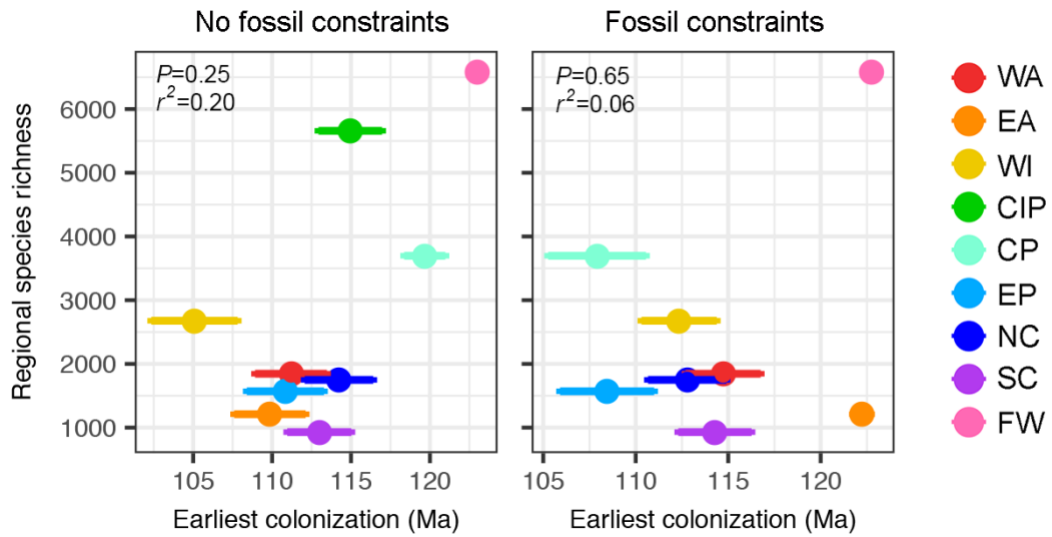

Figure S6. Regression between regional richness and the earliest colonization of a region, in reconstructions with and without fossil constraints. Values are the means across 100 stochastic maps; horizontal bars are the confidence intervals. In reconstructions with fossil constraints, colonizations to the CIP were forced to occur at 34 Ma or later. Thus, we removed the CIP from analysis. Results are not significant with $P<0.05$.

Table S7. Effect of increased taxon sampling on relationships between colonization and richness in Labridae. Significance values for log-transformed regional richness and either summed time or the number of colonizations, for phylogenies of Labridae with increasing levels of phylogenetic sampling. Values represent the means across 100 stochastic maps, for the two trees with genetic data only (published in 2013 and 2018). For ATA trees, values represent the means-of-means among 67 phylogenies (denoted with *; each phylogeny is represented by a mean across 100 stochastic maps). Note that we could only perform successful stochastic maps on 67 of 100 ATA trees. Note that our usage of Labridae here includes Scaridae and Odacidae.

Phylogeny	Number of species of Labridae	Number of trees with stochastic map simulations	Summed time		Number of colonizations	
			Mean *P*-value	Mean r^2	Mean *P*-value	Mean r^2
2013 [12]	244	1	0.047	0.714	0.010	0.863
2018, genetic data only [16]	339	1	0.027	0.773	0.002	0.931
2018, all taxa added [16]	630	67 of 100 trees	0.013*	0.832*	0.001*	0.970*

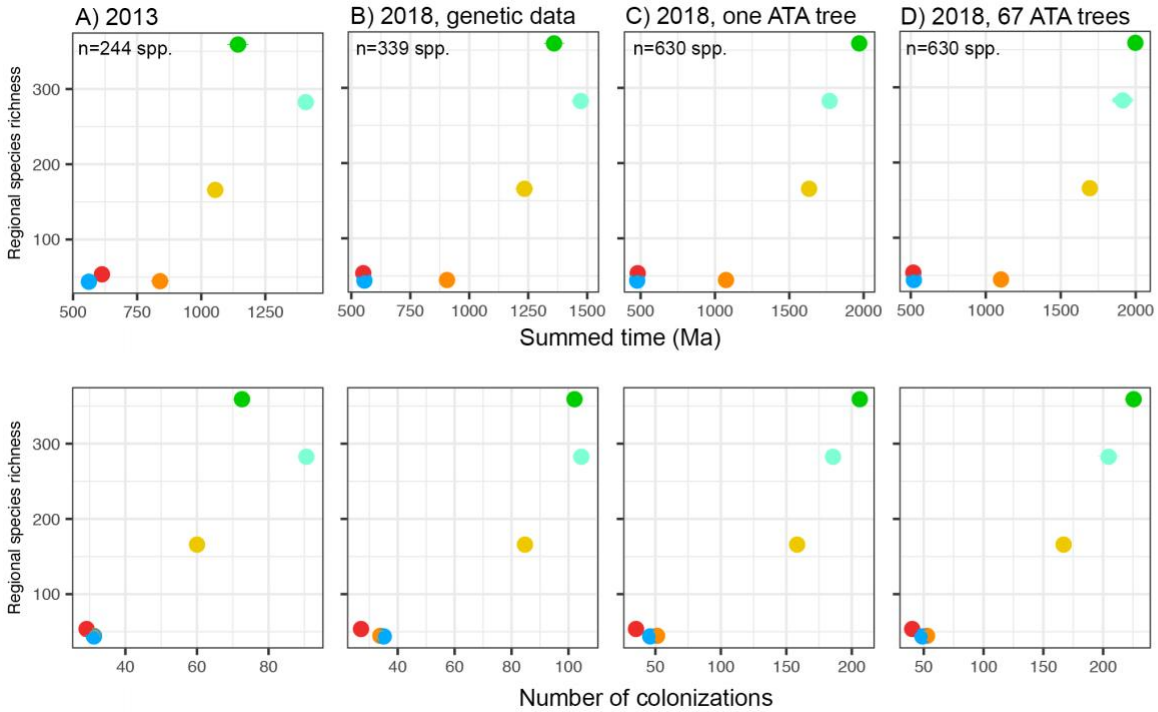

Region	Total	2013	2018
WA	54	41 (76%)	44 (81%)
EA	45	32 (71%)	34 (76%)
WI	166	65 (39%)	102 (61%)
CIP	359	141 (39%)	191 (53%)
CP	283	133 (47%)	179 (63%)
EP	44	23 (52%)	38 (86%)

Figure S7. Differences in colonization results in Labridae using phylogenies published in (A) 2013 [12], (B) 2018 with genetic data only [16], and (C–D) 2018 with all taxa added semi-randomly with taxonomic constraints ("ATA" trees of [16]). Column C depicts results for ATA tree 1 of 100 only; column D depicts means across 67 ATA trees. Points in columns A–C show the mean values for each region from 100 stochastic simulations based on the fitted biogeographic model on a single phylogeny. Points in column D represent means-of-means among 67 phylogenies (each phylogeny is represented by a mean value from 100 stochastic simulations). Horizontal bars show the confidence intervals associated with means, but are generally too narrow to be visible. Note that we could only successfully perform stochastic simulations of biogeography on 67 of 100 ATA trees (column D). Table inset shows the proportion of species with genetic data from each region sampled among the phylogenies. Wrasse photograph: *Thalassoma lunare*, Leonard Low (Wikimedia creative commons attribution 2.0 generic license).

References

1. Ree RH, Smith SA. 2008 Likelihood inference of geographic range evolution by dispersal, local extinction, and cladogenesis. *Syst. Biol.* **57**, 4–14.
2. Matzke NJ. 2014 Model selection in historical biogeography reveals that founder-event speciation is a crucial process in island clades. *Syst. Biol.* **63**, 951–970.
3. Massana KA, Beaulieau JM, Matzke NJ, O'Meara BC. 2015 Non-null effects of the null range in biogeographic models: exploring parameter estimation in the DEC model. *bioRxiv* (doi: https://doi.org/10.1101/026914).
4. Palumbi SR. 1994 Genetic divergence, reproductive isolation, and marine speciation. *Annu. Rev. Ecol. Syst.* **25**, 547–572.
5. Burnham KP, Anderson DR. 2002 Information and likelihood theory: a basis for model selection. In *Model Selection and Multimodel Inference* (Burnham KP, Anderson DR), pp 49–97. New York, NY:Springer-Verlag.
6. Cowman PF, Bellwood DR. 2013 The historical biogeography of coral reef fishes: global patterns of origination and dispersal. *J. Biogeogr.* **40**, 209–224.
7. Dornburg A, Moore J, Beaulieu JM, Eytan RI, Near TJ. 2014 The impact of shifts in marine biodiversity hotspots on patterns of range evolution: Evidence from the Holocentridae (squirrelfishes and soldierfishes). *Evolution* **69**, 146–161.
8. Floeter SR *et al.* 2008 Atlantic reef fish biogeography and evolution. *J. Biogeogr.* **35**, 22–47.
9. Vermeij GJ, Dudley R. 2000 Why are there so few evolutionary transitions between aquatic and terrestrial ecosystems? *Biol. J. Linn. Soc.* **70**, 541–554.
10. Bellwood DR, Goatley CHR, Bellwood O. 2017 The evolution of fishes and corals on reefs: form, function, and interdependence. *Biol. Rev.* **92**, 878–901.
11. Renema W *et al.* 2008 Hopping hotspots: global shifts in marine biodiversity. *Science* **321**, 654–657.
12. Rabosky DL, Santini F, Eastman J, Smith SA, Sidlauskas B, Chang J, Alfaro ME. 2013 Rates of speciation and morphological evolution are correlated across the largest vertebrate radiation. *Nat. Commun.* **4**, 1958.
13. Bannikov, A.F. 2014. The systematic composition of the Eocene actinopterygian fish fauna from Monte Bolca, northern Italy, as known to date. *Studi e Ricerche sui Giacimenti Terziari di Bolca* **12**, 23–34.
14. Matzke NJ. 2015 Stochastic mapping under biogeographical models. See http://phylo.wikidot.com/biogeobears#stochastic_mapping/.
15. Stephens P.R., Wiens J.J. 2003. Explaining species richness from continents to communities: the time-for-speciation effect in emydid turtles. *Am. Nat.* **161**, 112–128.
16. Rabosky DL, Chang J, Title PO, Cowman PF, Sallan L, et al. 2018 An inverse latitudinal gradient in speciation rate for marine fishes. *Nature* **559,** 392–395.
17. Barber PH, Bellwood DR. 2005 Biodiversity hotspots: evolutionary origins of biodiversity in wrasses (Labridae) in the Indo-Pacific and New World tropics. *Mol. Phylogenet. Evol.* **35**, 235–253.
18. Cowman PF, Bellwood DR. 2013 The historical biogeography of coral reef fishes: global patterns of origination and dispersal. *J. Biogeogr.* **40**, 209–224.
19. Rabosky DL. 2015 No substitute for real data: A cautionary note on the use of phylogenies from birth-death polytomy resolvers for downstream comparative analyses. *Evolution* **69,** 3207–3216.